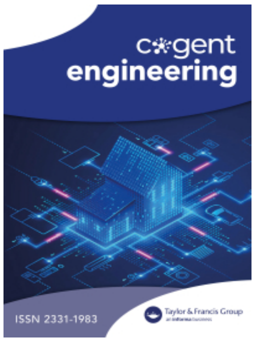

Taylor & Francis
Taylor & Francis Group

Cogent Engineering

ISSN: (Print) (Online) Journal homepage: www.tandfonline.com/journals/oaen20

Microstructure and surface characterization of copper and zinc added heat treated stir cast A356 alloy

Nithesh K., Sathyashankara Sharma, Gowrishankar M. C., Rajesh Nayak, Ananda Hegde, Rajesh Bhat & Karthik B. M.

To cite this article: Nithesh K., Sathyashankara Sharma, Gowrishankar M. C., Rajesh Nayak, Ananda Hegde, Rajesh Bhat & Karthik B. M. (2024) Microstructure and surface characterization of copper and zinc added heat treated stir cast A356 alloy, Cogent Engineering, 11:1, 2371530, DOI: 10.1080/23311916.2024.2371530

To link to this article: https://doi.org/10.1080/23311916.2024.2371530

Published online: 28 Jun 2024.

COGENT ENGINEERING
2024, VOL. 11, NO. 1, 2371530
https://doi.org/10.1080/23311916.2024.2371530

cogent

MATERIAL ENGINEERING | RESEARCH ARTICLE

OPEN ACCESS Check for updates

Microstructure and surface characterization of copper and zinc added heat treated stir cast A356 alloy

Nithesh K.[a,b], Sathyashankara Sharma[b], Gowrishankar M. C.[b], Rajesh Nayak[b], Ananda Hegde[b], Rajesh Bhat[c] and Karthik B. M.[b]

[a]Department of Mechanical Engineering, A J Institute of Engineering &Technology, Mangalore, India; [b]Department of Mechanical and Industrial Engineering, Manipal Institute of Technology, Manipal Academy of Higher Education, Manipal, India; [c]Department of Aeronautical Engineering, Srinivas Institute of Technology, Mangalore, India

ABSTRACT

The aim of this work is to investigate the variations in microstructure, hardness, wear and surface roughness between as-cast and heat treated trace elements added A356 alloy. Alloy A was prepared by adding 1 wt.% magnesium to A356 alloy which was used as the base material for the preparation of alloys with zinc (Zn) and copper (Cu) particles as alloying elements. Other set of samples was fabricated where Cu-coated Zn and Cu were added as reinforcements to base matrix A. The microstructural analysis indicated that the addition of Zn to A356 as an alloying element had a limited effect on controlling the grain size during solidification compared to Cu. The addition of Cu as reinforcement resulted in a higher proportion of pro eutectic α-Al phase, leading to finer grain boundaries. Micro-polishing test was conducted on the alloys and composites by determining the surface roughness (Ra) value using profilometer to study the changes in surface roughness under individual load conditions of 20 and 40 N. In the as-cast condition, the addition of Cu increased the hardness by 39% and 58% over the base alloy, respectively. Age-hardening treatment significantly enhanced the wear resistance properties of unreinforced alloys and composites at both aging temperatures, especially at 100 °C. Composite samples exhibited excellent surface finish (lower surface roughness) compared to alloy samples, attributed to the presence of hard reinforcement particles.

ARTICLE HISTORY
Received 7 April 2024
Revised 17 June 2024
Accepted 18 June 2024

KEYWORDS
Microstructure; surface characterization; aluminum alloy

REVIEWING EDITOR
Dr Ian Phillip Jones, Metallurgy & Materials, University of Birmingham, United Kingdom of Great Britain and Northern Ireland

SUBJECTS
Metals & Alloys; Materials Processing; Manufacturing Engineering

Introduction

The revolution of composites as an important class of materials for humankind has shown remarkable results in tracking the background and history of composites, from the ancient natural category to the development of modern synthetic materials such as fiberglass. The components of composites have been studied, highlighting the presence of reinforcement phases embedded within matrix materials such as metals or polymers (Hunt, 2000; Davis, 2001). By focusing specifically on metal matrix composites (MMCs) and emphasizing the use of metals such as aluminum (Al) alloys as matrices, it is possible to balance the specific strength and surface characteristics (Nithesh et al., 2023; Miyajima & Iwai, 2003; Kashimat et al., 2023). Moreover, it is necessary to explore the significance of alloying elements and reinforcement materials, particularly copper (Cu) and zinc (Zn) powders, which contribute to the precipitation hardening process that strengthens the alloy and composites. Coatings play a vital role in enhancing the performance of composites, and in contrast, the aging dynamics of composites at high temperatures are accelerated compared to Al alloys used as matrices (Zhang et al., 2015; Mandal et al. 2008; Bhav Singh and Balasubramanian, 2009). The presence of high-density dislocations in composites leads to the faster development of new phases through thermal processes. Several researchers have attempted to study the effects of Cu and Zn addition to Al–Si alloys. Shabestari and Moemeni (2004) studied the microstructure and mechanical properties of A356 alloys

CONTACT Sathyashankara Sharma ss.sharma@manipal.edu Department of Mechanical and Industrial Engineering, Manipal Institute of Technology, Manipal Academy of Higher Education, Manipal, Karnataka, India

with Cu contents varying between 0.2 and 2.5 wt.%. They found that adding 1.5 wt.% Cu improved mechanical properties, with high cooling rate significantly increasing the strength and hardness values. Cai et al. (2016) found that an increase in Cu wt.% to Al-Si_p strengthened the composite, increasing hardness and wear resistance. However, up to 2 wt.% Cu increased mechanical properties, while further increase decreased the properties. Yadav and Bauri (2015) studied the friction stir casting method for high-solubility Cu reinforcement in a pure Al matrix, revealing an improved strength, ductility and thermal stability above 300 °C. Saito et al. (2014) investigated the effect of adding Zn to Al–Mg–Si alloys and analyzed their microstructure and intergranular corrosion behavior. The results showed minor increases in hardness and increased needle-shaped precipitates; however, no precipitates were found in the Al–Zn–Mg alloy system. The Zn-rich layer increased sensitivity to intergranular corrosion. Alemdağ and Beder (2014) found that the addition of Zn to Al-7Si-(0–5) Zn alloys increased the size and volume fraction of the primary Si particles, forming an α-solid solution and increasing the tensile strength, hardness and density. However, increasing the Zn content in the Al-12Si-Cu alloy increased the ductility, hardness and tensile properties but decreased the friction and wear rate (Alemdag and Beder, 2019). The aim of this study is to investigate the variations in the surface roughness, hardness and microstructure of as-cast and heat-treated A356 alloys and composites. The properties were studied with trace additions of Cu and Zn as alloying elements, and Cu-coated Zn and Cu as reinforcements to the A356 alloy. The novelty of this work is the addition of a lower melting point reinforcement (Zn) into the matrix and efforts to explore the dual role (alloy and reinforcement) of Cu and Zn in property enhancement.

Experimental details

This study used A356 alloy ingots purchased from Laxmi Metal Exchange, Coimbatore and Mg, Zn and Cu powders were procured from Siltech Corporation, Bangalore. Chemical analysis on the procured material was done according to ASTM E-1521-2011 standards and particle size analysis revealed average particle sizes of Cu and Zn as 9.33 and 33 μm, respectively. The experimental procedure involved melting the A356 ingots at 750 °C in an electric resistance furnace, followed by the addition of 1 wt.% Mg to increase age-hardening characteristics and wettability. Molten metal was poured into preheated molds to form as-cast alloy A bars, which served as the foundation for the subsequent alloys and composites, including Cu and Zn additions. Alloy A1 was prepared using the mechanical stir-casting method, by adding 0.5 wt.% Zn and Cu particles each as alloying elements. After degassing, the alloy was transferred into the prepared molds to form as-cast A1 alloys. The same technique was used for the preparation of the as-cast A2 alloy with 1 wt.% Cu addition as alloying element without Zn.

The C1 composite was fabricated using alloy A as the matrix and adding 0.5 wt.% Cu-coated Zn and Cu as reinforcements using a two-step liquid-stir-casting technique. To maintain the distinct identity of Zn in the composite, a Cu coating with a thickness of 10–12 μm was applied using electrolytic Cu coating technique, ensuring that the Zn particles remained intact despite the low melting point of Zn (480 °C). The process involved melting Alloy A in a graphite crucible at a uniform temperature of 750 °C. The melt was then allowed to cool to 600 °C to form a semisolid state. At this stage, continuous stirring at 150–200 RPM was used to introduce the preheated Cu into the vortex. The molten metal and reinforcements were stirred to uniformly disperse them, and the temperature was raised to 750 °C with continuous stirring at 400 RPM. The molten alloy was poured into preheated molds to obtain the as-cast C1 composite. The same procedure was used for C2 composites with 1 wt.% Cu addition as reinforcement without Cu-coated Zn. Table 1 shows the designations of the alloys and composites along with respective compositions used in this study. Figure 1 shows the stir casting setup used for the fabrication of alloys and composites with trace amounts of Cu and Zn.

The age-hardening treatment of the A356 alloy and its composites involved solutionizing the material at 550 °C for 2 h, followed by water quenching. This process dissolved the harder Mg_2Si intermetallic phase, forming a homogenous single-phase matrix. The material was then aged at 100 °C and 200 °C to encourage the precipitation of the Mg_2Si phase along with the precipitation of other intermetallics, resulting in material strengthening. This process removes the continuous network of Mg_2Si precipitates along the grain boundary and spreads the same as discrete particles in both the grain boundary zone and within the grain (Sidney, 2004). Hardness measurements were performed at hourly intervals to determine the peak hardness value of the sample.

Table 1. Designations used in this study.

Material (wt%)	Designation	Type
A356 + 1% Mg alloy	A	Alloy
A + 0.5% Zn + 0.5% Cu alloy (Zn and Cu as alloying element)	A1	
A + 1% Cu alloy (Cu as alloying element)	A2	
A + 0.5% Cu-coated Zn + 0.5% Cu composite (Cu-coated Zn and Cu as reinforcement)	C1	Composite
A + 1% Cu composite (Cu as reinforcement)	C2	

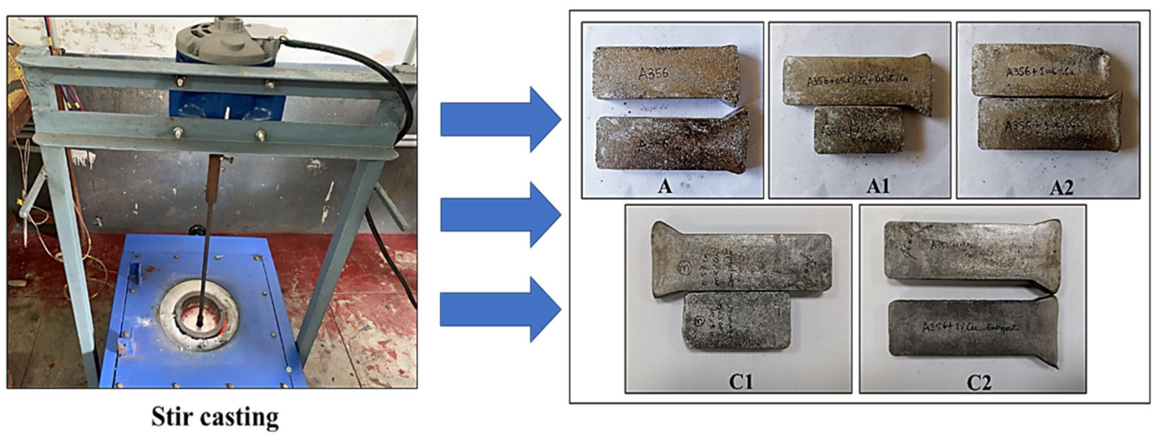

Figure 1. Experimental setup used for the preparation of alloys and composites.

Cubic specimens from the as-cast alloys and composites were polished, buffed and etched using Keller's reagent to analyze the microstructural changes. An inverted metallurgical optical microscope and a scanning electron microscope (SEM) equipped with Energy Dispersive X-ray microanalysis (EDX) were used to examine the microstructure and distribution of the reinforcing particles. A Matzusawa Vickers microhardness tester was used to measure the hardness of both the as-cast and age-hardened A356 alloys and composites with a load of 200 gmf and dwell time of 15 s. An average value of five concurrent hardness values was used to determine the hardness values, rejecting abnormal values.

A dry sliding wear test was conducted on a pin-on-disc tribometer according to ASTM G99 standards at an applied load of 60 N and sliding distance up to 3000 m. A specimen diameter of 8 mm was considered for the wear test, and the cumulative weight loss for each specimen was recorded at regular intervals of 500 m sliding distance. The test conditions are listed in Table 2. The wear rate W_r (mm^3/m) was obtained using Equation (1).

$$Wr = \frac{\Delta m}{S * \rho} \qquad (1)$$

where Δm – weight loss (mg) = Initial weight – Final weight

S – sliding distance (m) and ρ – experimental density.

Table 2. Test conditions for wear test.

Disc material	EN-31 steel, 65 HRC
Disc size	Φ100 mm × 6 mm thickness
Speed	200 RPM
Wear track diameter	60 mm
Testing environment	Dry sliding
Load	60 N
Sliding distance	0–3000 m
Initial surface roughness of pin	0.9 μm

A micro-polishing test was conducted on A1 and A2 alloys and C1 and C2 composites, comparing them with base alloy A. Test specimens were machined using the wire-EDM process, loaded into an automatic pneumatic mounting press, and Bakelite powder was added to form a mold. The mold was loaded onto the micropolishing holder using a metallographic grinding and polishing machine. The test specimens were polished on emery paper and finely polished using a diamond suspension. Individual loads of 20 and 40 N were applied to study the surface roughness changes. The surface roughness (Ra) was measured using a Surtronic 3+ profilometer with a sampling length of 4 mm.

Results and discussion

Microstructure

The optical microstructure images of alloy A (A356) revealed several features, showing α-Al phase distributed throughout the base alloy, including a refined microstructure with a finer eutectic colony and a well-dispersed pro-eutectic Al phase, particularly along the grain boundaries. Figure 2 shows the optical microstructure images representing the grain size and distribution of the phases. The grain size of the as-cast A1 alloy was larger than that of the A356 alloy without the addition of Zn and Cu, which could be related to the lower melting temperature of Zn. The presence of the pro-eutectic phase shows the importance of these alloying components in the final microstructural features of the A356 alloy, which affect mechanical properties, such as strength, ductility and wear resistance. The distribution of both eutectic and pro-eutectic phases in the A2 alloy is remarkable, resulting in a homogeneous distribution, which results in favorable material characteristics, such as enhanced strength, ductility and overall mechanical performance. The as-cast composite C1 showed moderate grain size structures; in contrast, the C2 composites showed a very fine grain structure, as shown in Figure 2. As the number and quantity of reinforcements increases, grains are becoming finer to increase heterogenous nucleation sites for the precipitation of stretching phases during controlled heat treatment. Accordingly, C1grains are finer than A1 and A2. C2 is still finer than the remaining specimens as seen in Figure 2. These fine grains resulted from a large temperature mismatch between Cu and alloy A. Comparing the respective composites and alloys, the alloy category showed a larger grain size structure. Figures 3 and 4 show the distribution and confirmation of the reinforcements in the C1 and C2 composites. The reinforcement distribution appeared homogeneous across the specimens.

Hardness variation

This study investigated the Vickers microhardness variation of alloy A with respect to the trace additions of Zn and Cu as alloying elements and reinforcements. Figure 5 depicts the increase in hardness values for the A1, A2, C1 and C2 samples. This increase in hardness was attributed to the differences in the size and shape of the eutectic Si particles, as well as the formation of various intermetallic phases. Compared to base alloy A, the hardness value increased by 16% and 39% in A1 and A2 alloy. With composite samples C1 and C2 having higher hardness values than the comparable alloys A1 and A2, Zn incorporation had a minimal effect on the improvement in hardness.

The hardness of the A356 composites was enhanced by 28% when 0.5 wt.% Cu coated Zn and Cu was added to alloy A and 58% when 1 wt.% Cu reinforcement was added alone. But 0.5 wt.% Zn addition did not contribute much as a solid-state strengthening phase and there was not enough wt.% of Mg and Zn available to create the necessary $MgZn_2$ intermetallic phase. Overall, 1 wt.% Cu-reinforced composite (C2) showed a significant increase in hardness value.

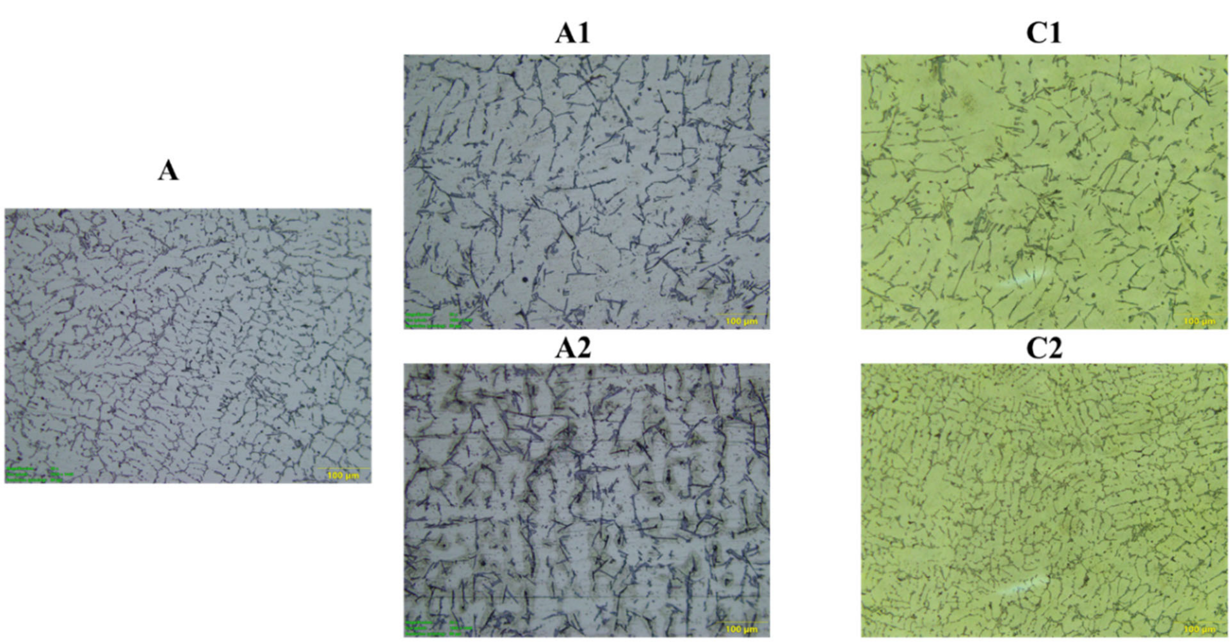

Figure 2. Optical microstructure images of alloys and composites at 100X.

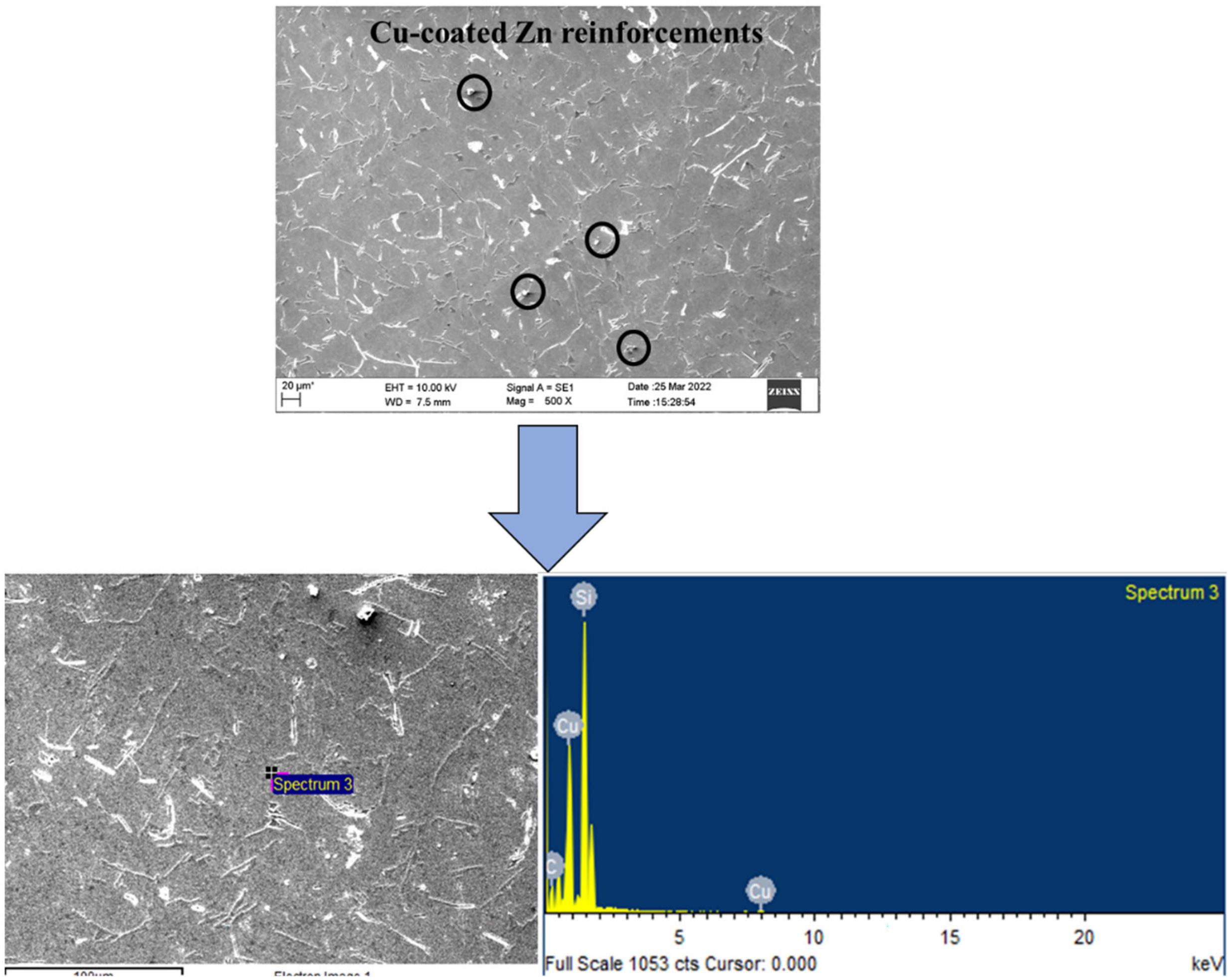

Figure 3. Reinforcement confirmation in C1 composite using EDX.

Effect of aging (T6) condition

The peak hardness values of the alloys and composites at different temperatures are presented in Figures 6 and 7, respectively. It was found that the hardness value increased with increasing aging time until the peak-aged condition. The addition of Cu was found to be responsible for the increase in the hardness value during the solutionizing and peak aging states, hence improving the solid solution strengthening of A356. By producing Mg_2Si intermetallic phases, the intentional addition of 1 wt.% magnesium increased the wettability in composites and strengthened A356 during solid solution. Addition of 0.5 wt.% Zn did not significantly affect the hardness improvement at peak aged condition, however the time required to attain peak aged condition decreased with increasing Cu wt.%. A lower aging temperature (100 °C) resulted in higher peak hardness values, although a longer time was required to achieve peak hardness than at 200 °C. Aging at 200 °C produced two peaks for each sample, the first of which had a lower hardness value than the second peak. The decreasing trend of the hardness value remained stable and did not increase after peak aging (2nd peak). This was due to the metastable transition state of the unevenly sized growing embryo into stable intermetallics, which resisted dislocation movement (Sidney, 2004). The GP zones initially formed homogeneously within the matrix, but the metastable phases resisted dislocation movement, resulting in a transient slowdown in the strengthening process at the first peak. The θ phase (Al_2Cu) exhibited greater hardness before peak aging. However, metastable phases may not have grown or may have been too small for effective dislocation interactions (Rajan et al., 2010).

Wear

Tribological applications require alloys and composites with low friction coefficients, high wear resistance and the ability to sustain heavy loads without

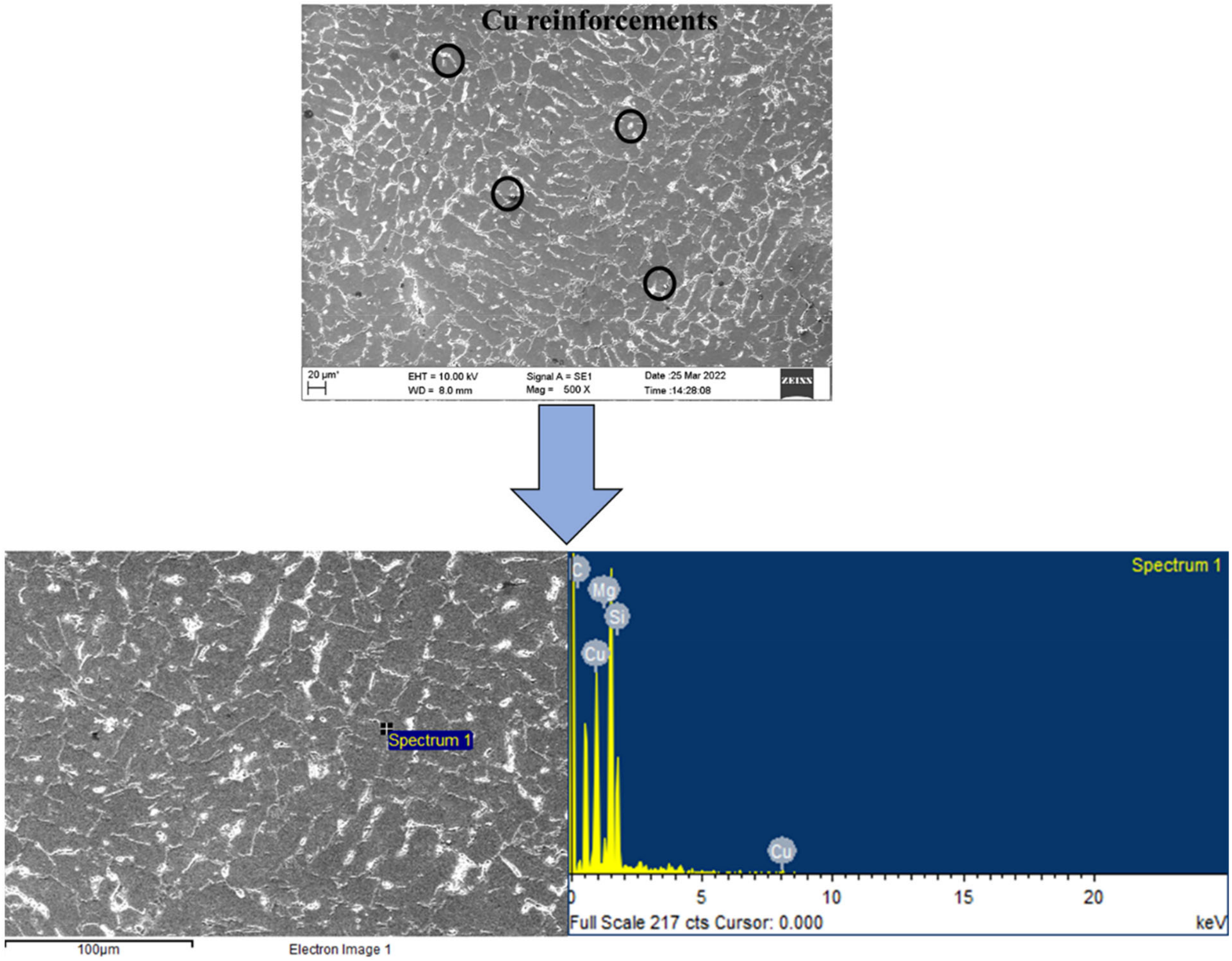

Figure 4. Reinforcement confirmation in C2 composite using EDX.

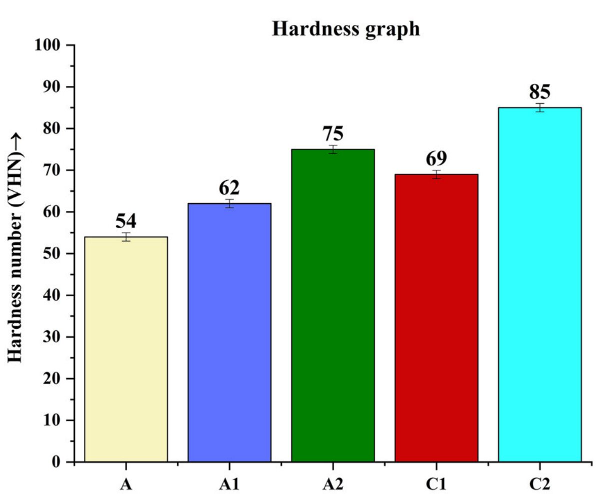

Figure 5. Hardness values of the alloys and composites.

breakdown, distortion or fracture. A number of external factors, such as alloying elements, mechanical deformation and heat treatment, may influence the specific strength and wear resistance of a material. Wear resistance is also influenced by working conditions such as temperature, sliding speed, sliding distance and applied load. Figures 8 and 9 show the variation in the wear rate (W_r) against the sliding distance for the as-cast and heat-treated samples at a load of 60 N. The wear resistance of the A356 alloy was improved by the addition of reinforcement or alloying elements. The addition of Cu may have resulted in greater wear resistance in the A2 alloy at higher sliding distances. Under as-cast conditions, W_r in the A2 alloy was observed in the range of 2.3–9.3*10^{-5} mm^3/m with increasing sliding distance. However, after age hardening treatment, W_r in the A2 alloy was significantly reduced to 0.5–4.4*10^{-5} mm^3/m. Similarly, the 100 °C peak-aged C2 composites showed a W_r of 0.4–4.3*10^{-5} mm^3/m. Samples that were peak-aged at 100 °C exhibited reduced wear, with Cu addition being responsible for the highest wear resistance in the respective alloy and composite categories. At an applied load of 60 N, the wear of composites C1 and C2 increased slightly owing to the increased plastic deformation, which led to wear particles. The presence of hard reinforcements in the C1 and C2 composites

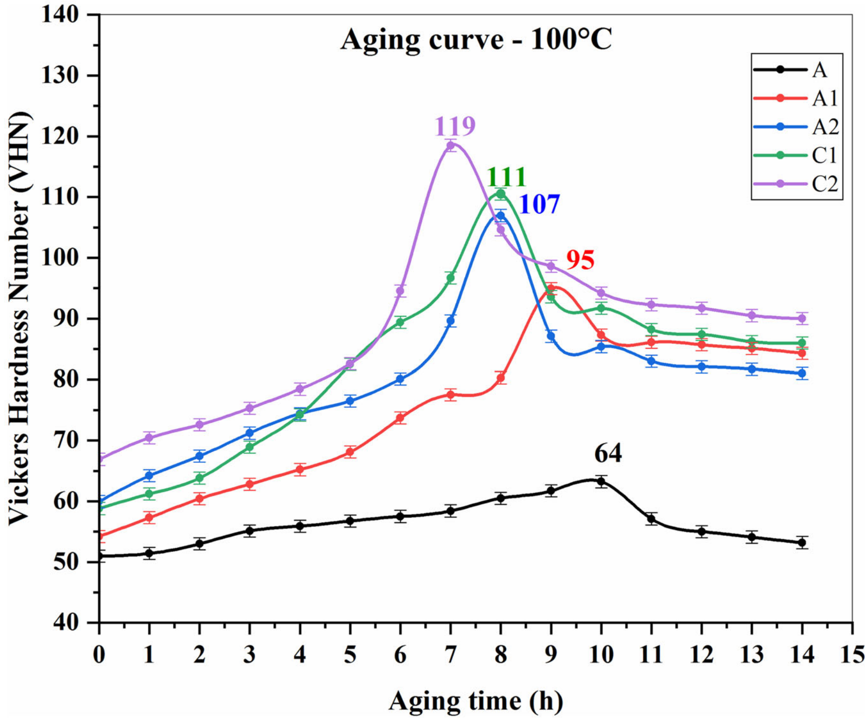

Figure 6. Peak aging graph at 100 °C for alloys and composites.

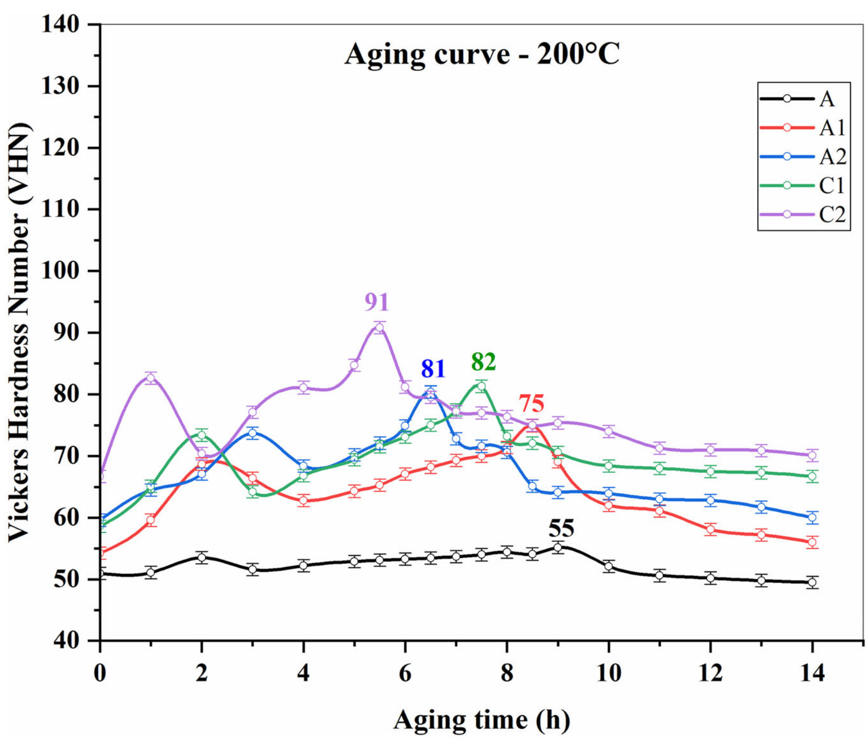

Figure 7. Peak aging graph at 200 °C for alloys and composites.

supports the contact stresses and prevents high plastic deformation and abrasion between the contact surfaces. The C2 composite showed better wear resistance even at higher loads and sliding distances, possibly owing to the addition of 1 wt.% Cu reinforcement to alloy A. Age hardening treatment improved wear resistance properties in unreinforced alloy A and its composites.

The measured friction and normal forces were used to calculate the coefficient of friction. The test

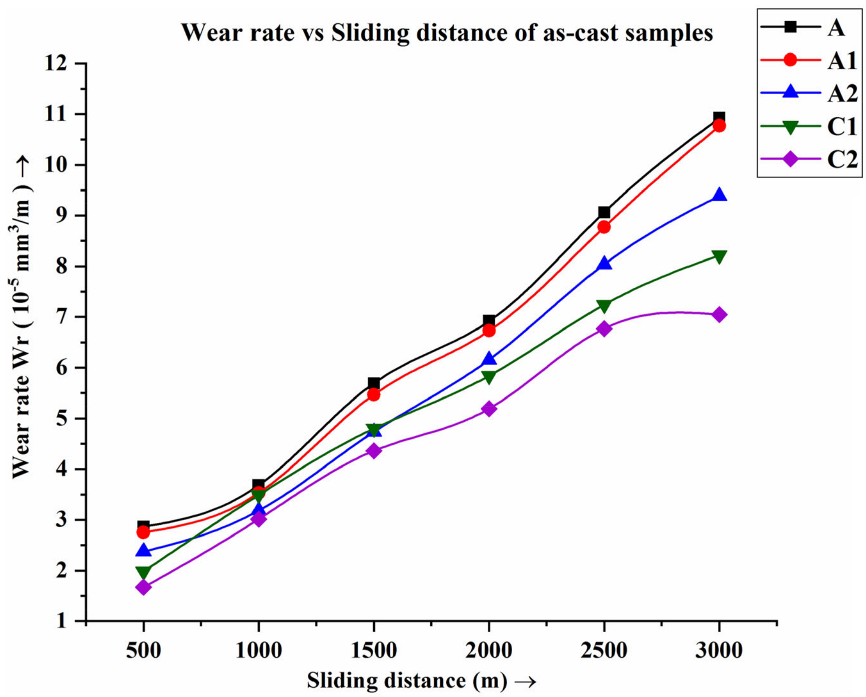

Figure 8. Wear rate graph of as-cast alloys and composite at applied load of 60 N.

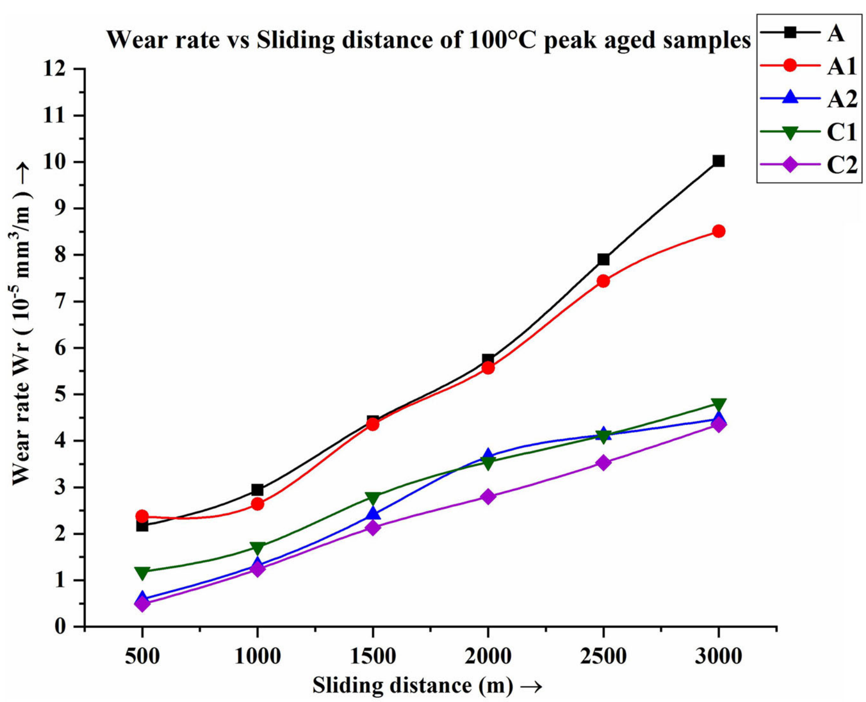

Figure 9. Wear rate graph of peak aged alloys and composite at applied load of 60 N.

results showed that there was an initial phase in each case, during which the coefficient of friction significantly dropped, followed by a stable state with almost constant friction. At a load of 60 N, Figures 10 and 11 show the coefficient of friction against the sliding distance curves for the as-cast and peak-aged alloys and composites. Under the as-cast condition, the lowest average coefficient of friction of roughly 0.74–0.78 was found in the respective alloy category, whereas the average coefficient of friction of the composites was 0.32–0.42. The composite samples showed significantly lower coefficients of friction than the respective alloy categories. The development of a mechanically mixed layer

(MML) lowered the friction between mating surfaces, which could be the cause of the observed trend. Wear debris may have resulted from MML disruption as the load increased.

Comparison of surface roughness value

Micro-polishing is a finishing technique that employs fine abrasive particles to smooth and refine the surface of a material (Khomamizadeh & Ghasemi, 2004). This can reduce the surface roughness of the A356 alloy by removing imperfections and burrs, thereby improving the surface finish and corrosion resistance. The surface roughness (Ra) varies according to the applied stress, with increasing load resulting in surface compression and decreasing roughness (Bhattacharjee et al., 2014). The Ra values of the prepared alloys and composites were determined in the as-cast and heat-treated conditions under load conditions of 20 and 40 N.

Figures 12 and 13 show the surface roughness (R_a) value of alloys and composites at 20 and 40 N. Under the load condition of 20 N, as-cast alloy A exhibited the highest Ra value of 0.82 μm, whereas as-cast alloys A1 and A2 showed Ra values of 0.76 and 0.7 μm, respectively. The surface roughness of alloy A may have been affected by the applied load, leading to the plastic deformation and increased roughness. In contrast, the addition of a small quantity of Cu (0.5 wt.% in A1 and 1 wt.% in A2) reduced the Ra value, resulting in better surface roughness under both as-cast and lower load conditions. The Ra values of as-cast alloys A, A1, and A2 decreased to 0.8, 0.7 and 0.66 μm, respectively, as the applied load increased from 20 to 40 N. Increased plastic deformation may be the cause of the decrease in surface roughness under higher loads, which could lead to an uneven and more irregular surface with a lower Ra value. The alloy deformed and strengthened with an increase in load, improving the surface quality. Under a load of 40 N, as-cast alloy A2 displayed the lowest Ra value of 0.66 μm.

The Ra values were significantly lower for the 100 °C peak-aged samples than for the as-cast samples under similar loading conditions. Peak aging strengthens and hardens the alloy, reducing its susceptibility to plastic deformation and resulting in smoother surfaces. Aging of the alloys and composites produced smoother surfaces by refining α-Al and eutectic Si. Alloys A, A1 and A2 had Ra values of 0.4, 0.32 and 0.27 μm respectively, at peak-aged conditions at a load of 40 N.

Comparatively, composite samples C1 and C2 exhibited even lower Ra values under the studied conditions. Under a 20 N load, as-cast C1 and C2 composites showed Ra values of 0.5 and 0.39 μm, respectively, while under a 40 N load, the Ra values decreased to 0.43 and 0.39 μm, respectively. The lower Ra values in composites C1 and C2 compared to alloys A1 and A2 can be attributed to the combination of hard reinforcement particles, which deform more during micropolishing. The hard Cu

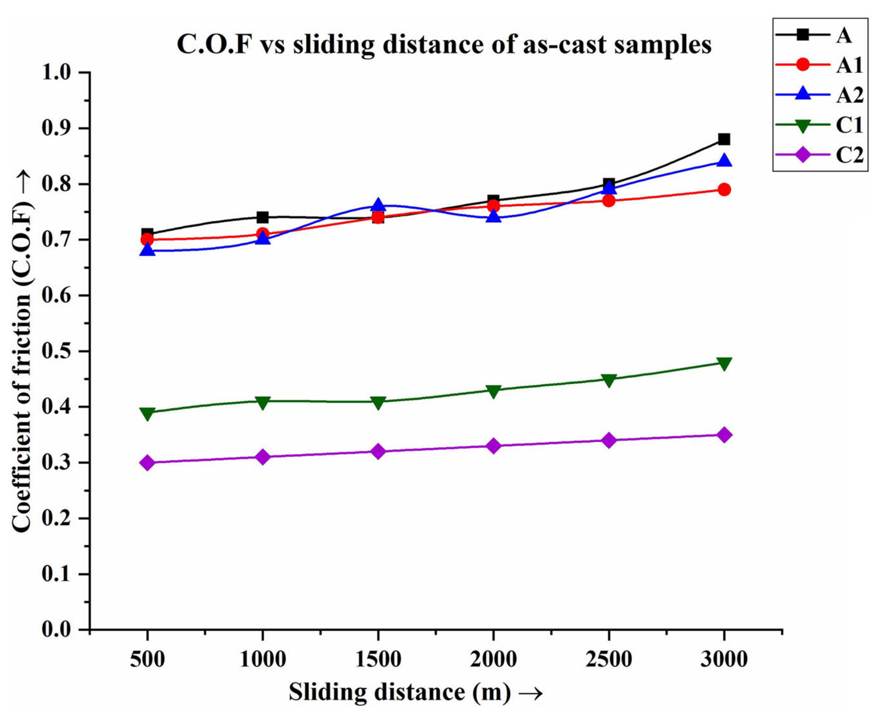

Figure 10. C.O.F graph of as-cast alloys and composites at applied load of 60 N.

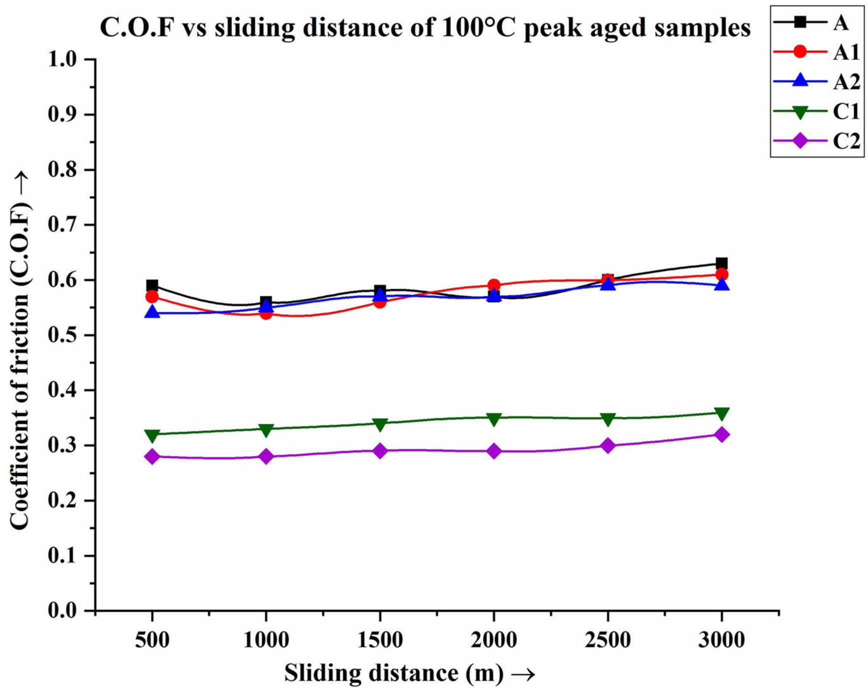

Figure 11. C.O.F graph of peak aged alloys and composites at applied load of 60 N.

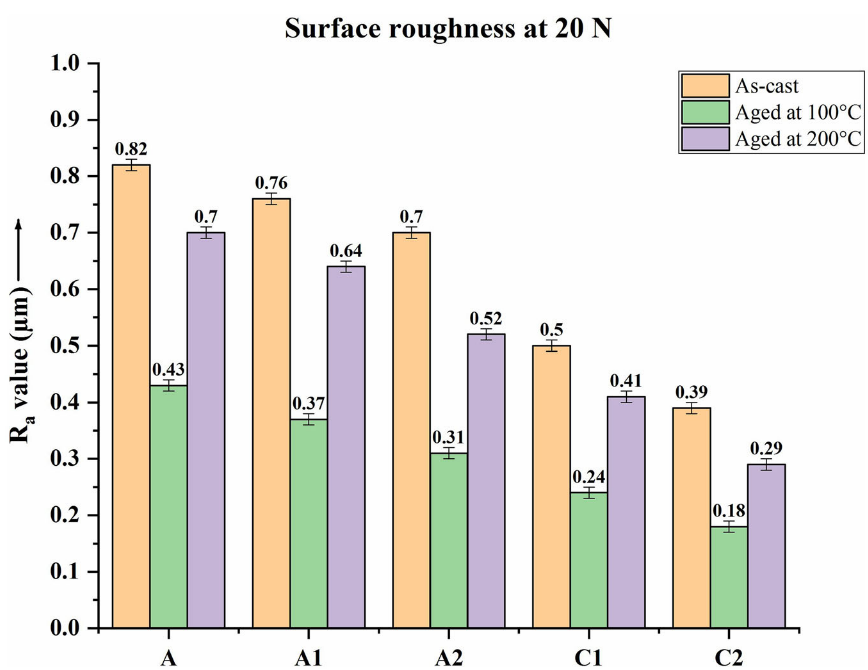

Figure 12. Surface roughness R_a value of alloys and composites at 20 N.

and Cu-coated Zn particles in the composites act as abrasive agents, smoothing the surface and leading to more deformation during micropolishing, further reducing the surface roughness.

Conclusions

Age-hardening treatment at 100 °C significantly improved the peak hardness and wear resistance of all alloys and composites, thereby reducing the chances of plastic deformation and resulting in smoother surfaces. The conclusions are summarized as follows:

- The successful incorporation of Cu-coated Zn particles into the A356 alloy through a two-step stir casting process demonstrated the feasibility of using a lower melting point reinforcement (Zn) in

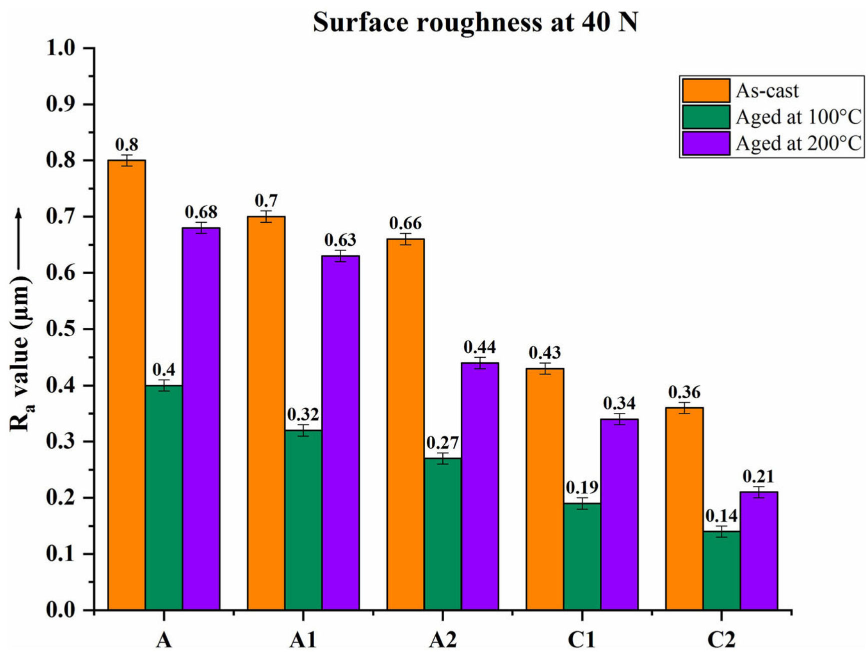

Figure 13. Surface roughness R_a value of alloys and composites at 40 N.

a higher melting point matrix to fabricate A356 composites.

- Microstructural analysis indicated that although the addition of Zn to A356 as an alloying element had a limited effect on controlling the grain size during solidification, the addition of 1 wt. % Cu as an alloying element resulted in a higher proportion of pro eutectic α-Al phase, leading to finer eutectic colony of Al–Si. As the number and quantity of alloying elements/reinforcements increases, grains are becoming finer to increase heterogenous nucleation sites.
- The addition of 1 wt.% Cu as an alloying element to A356 alloy resulted in a maximum hardness of 75 VHN, while in the as-cast composites, the maximum hardness of 85 VHN was achieved with the addition of 1 wt.% Cu reinforcement to A356 alloy. Moreover, the hardness distribution along the surface of the as-cast alloy and composite was found to be uniform, with a difference of ±3 VHN.
- The addition of 1 wt.% Cu exhibited maximum wear resistance in the corresponding alloy and composite categories. The age-hardening treatment significantly enhanced the wear resistance properties of unreinforced alloy A and its composites.
- The addition of small quantities of Cu to alloys A1 and A2 resulted in better surface roughness under lower load conditions, highlighting the importance of alloy composition in surface quality improvement.
- Peak aging at 100 °C significantly improved the surface roughness of all the alloys by increasing their strength and hardness, thereby reducing the chances of plastic deformation and resulting in smoother surfaces.
- Composite samples C1 and C2 exhibited excellent surface finish (lower surface roughness) compared to alloy samples A1 and A2, attributed to the presence of hard reinforcement particles that act as abrasive agents, smoothing the surface and causing more deformation during micropolishing.

Acknowledgments

Not applicable.

Author’s contributions

Nithesh K and Sathyashankara Sharma: Writing original draft Preparation, Visualization.

Gowrishankar M. C. and Rajesh Nayak: Conceptualization, Methodology, Investigation;

Ananda Hegde and Rajesh Bhat; Resources, Validation, Review; Karthik B. M.: Review & Editing.

Consent for publication

The authors confirm that the work described has not been published.

Disclosure statement

The authors declare no competing interests.

Funding

No funding was received for this study.

About the authors

Dr Nithesh K is working as Assistant Professor in the Department of Mechanical Engineering, A J Institute of Engineering & Technology, Mangalore, He holds B.E. (Mechanical), M.Tech (Manufacturing Engineering) and Ph.D. (Mechanical Engineering) degrees. He has published 6 papers in journals and conferences. His area of interest includes heat treatment of metals.

Dr. Sathyashankara Sharma is working as Senior Professor and Head in the Department of Mechanical & Industrial Engineering, MIT, MAHE, Manipal. He holds B.E. (Mechanical), M.Tech. (Materials Engineering) and Ph.D. (Materials Engineering) degrees. He has more than 35 years of teaching experience. His area of interest includes materials engineering, heat treatment of metals and composites and deformation behavior of metals and composites. He has published more than 150 papers in journals and conferences.

Dr. Gowri Shankar, holds a Ph.D. from the Manipal Institute of Technology, and currently is a Professor at the Department of Mechanical and Industrial Engineering of the same institute. His main areas of research include Machining of Materials; Heat Treatment of Ferrous and Non-Ferrous Materials.

Dr. Rajesh Nayak, holds a Ph.D. from the Manipal Institute of Technology, and currently is an Associate Professor at the Department of Mechanical and Industrial Engineering of the same institute. His main areas of research include Machining of Materials, Cryogenic machining, Composite materials, Heat Treatment of Ferrous and Non-Ferrous Materials.

Dr. Ananda Hegde is working as Associate Professor in the Department of Mechanical & Industrial Engineering, MIT, MAHE, Manipal. He has more than 10 years of teaching experience. His area of interest includes materials engineering, heat treatment of metals. He has published more than 30 papers in journals and conferences.

Dr. Rajesh Bhat, holds PhD degree from Manipal Institute of Technogy, Manipal. His research interest includes aluminum composites.

Dr. Karthik B M, holds PhD degree from Manipal Institute of Technogy, Manipal. He is working as assisting professor at MIT Manipal. His research includes age hardening of alloys and characterization.

ORCID

Nithesh K. http://orcid.org/0009-0006-6843-5184
Sathyashankara Sharma http://orcid.org/0000-0001-8995-1563
Gowrishankar M. C. http://orcid.org/0000-0001-9951-800X
Ananda Hegde http://orcid.org/0000-0002-8256-8665
Karthik B. M. http://orcid.org/0000-0002-5769-9874

Data availability statement

Corresponding author agrees to share the data upon reasonable request.

References

Alemdag, Y., & Beder, M. (2019). Effects of zinc content on strength and wear performance of Al − 12Si − 3Cu based alloy. *Transactions of Nonferrous Metals Society of China*, *29*(12), 2463–2471. https://doi.org/10.1016/S1003-6326(19)65154-X

Alemdağ, Y., & Beder, M. (2014). Microstructural, mechanical and tribological properties of Al-7Si-(0. Zn alloys. *Materials and Design*, *63*(3), 159–167. https://doi.org/10.1016/j.matdes.2014.06.006

Bhattacharjee, D., Muthusamy, K., & Ramanujam, S. (2014). Effect of load and composition on friction and dry sliding wear behavior of tungsten carbide particle-reinforced iron composites. *Tribology Transactions*, *57*(2), 292–299. https://doi.org/10.1080/10402004.2013.870272

Bhav Singh, B., & Balasubramanian, M. (2009). Processing and properties of copper-coated carbon fibre reinforced aluminium alloy composites. *Journal of Materials Processing Technology*, *209*(4), 2104–2110. https://doi.org/10.1016/j.jmatprotec.2008.05.002

Cai, Z., Zhang, C., Wang, R., Peng, C., & Wu, X. (2016). Effect of copper content on microstructure and mechanical properties of Al/Sip composites consolidated by liquid phase hot pressing. *Materials and Design*, *110*, 10–17. https://doi.org/10.1016/j.matdes.2016.07.085

Davis, J. R. (2001). Surface engineering for corrosion and wear resistance. *ASM International*, *4*(1), 1–10. https://doi.org/10.1361/secw2001p001

Hunt, W. H. Jr., (2000). Aluminum metal matrix composites today. *Materials Science Forum*, *331–337*(10), 71–84. https://doi.org/10.4028/www.scientific.net/MSF.331-337.71

Kashimat, N., Sharma, S., Nayak, R., Manjunathaiah, K. B., Shettar, M., & Chennegowda, G. M. (2023). Experimental investigation of mechanical property and wear behaviour of T6 Treated A356 alloy with minor addition of copper and zinc. *Journal of Composites Science*, *7*(4), 149. https://doi.org/10.3390/jcs7040149

Khomamizadeh, F., & Ghasemi, A. (2004). Evaluation of quality index of A-356 aluminum alloy. *Statistical Center of Iran*, *11*(4), 386–391.

Mandal, D., Dutta, B. K., & Panigrahi, S. C. (2008). Effect of copper and nickel coating on short steel fiber reinforcement on microstructure and mechanical properties of aluminium matrix composites. *Materials Science and Engineering: A*, *492*(1–2), 346–352. https://doi.org/10.1016/j.msea.2008.03.031

Miyajima, T., & Iwai, Y. (2003). Effects of reinforcements on sliding wear behavior of aluminum matrix composites. *Wear*, *255*(1–6), 606–616. https://doi.org/10.1016/S0043-1648(03)00066-8

Nithesh, K., Nayak, R., Hande, R., Sharma, S., Gowri Shankar, M. C., & Doddapaneni, S. (2023). Dual role of trace elements in magnesium dissolved age hardened A356 alloy on microstructure and peak micro hardness. *Manufacturing Review*, *10*, 5–14. https://doi.org/10.1051/mfreview/2023003

Rajan, T. V., Sharma Rajan , T. V., Sharma, A. K., Sharma, C. P., & Sharma, A. (2010). *Heat treatment principles and techniques* (2nd ed.).

Saito, T., Wenner, S., Osmundsen, E., Calin, D., Andersen, S. J., & Røyset, J. (2014). *The effect of Zn on precipitation in Al – Mg – Si alloys*, Materials Science and Technology, No, 37–41. https://doi.org/10.1080/14786435.2014.913819

Shabestari, S. G., & Moemeni, H. (2004). Effect of copper and solidification conditions on the microstructure and mechanical properties of Al-Si-Mg alloys. *Journal of Materials Processing Technology*, *153–154*(1–3), 193–198. https://doi.org/10.1016/j.jmatprotec.2004.04.302

Sidney, H. A. (2004). *Introduction to physical metallurgy* (4th ed.). McGraw Hill.

Yadav, D., & Bauri, R. (2015). Development of Cu particles and Cu core-shell particles reinforced Al composite. *Materials Science and Technology*, *31*(4), 494–500. https://doi.org/10.1179/1743284714Y.0000000644

Zhang, Y., Zong, B. Y., Jin, J., & Cao, X. (2015). Electroless copper plating on particulate reinforcements and effects on mechanical properties of SiCp/Fe composite. *Surface Engineering*, *31*(3), 232–239. https://doi.org/10.1179/1743294414Y.0000000370